
Article:
Colantuono, G and Cockerill, T orcid.org/0000-0001-7914-2340 (2017) Selective strategy for solid sorbent replacement in CCS. Chemical Engineering Research and Design, 120. pp. 82-91. ISSN 0263-8762

https://doi.org/10.1016/j.cherd.2017.01.030

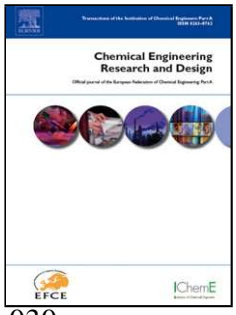

Title: Selective strategy for solid sorbent replacement in CCS

Author: Giuseppe Colantuono Timothy Cockerill

PII: S0263-8762(17)30083-7
DOI: http://dx.doi.org/doi:10.1016/j.cherd.2017.01.030
Reference: CHERD 2560

To appear in:

Received date: 4-10-2016
Revised date: 25-1-2017
Accepted date: 30-1-2017

Please cite this article as: Giuseppe Colantuono, Timothy Cockerill, Selective strategy for solid sorbent replacement in CCS, *<![CDATA[Chemical Engineering Research and Design]]>* (2017), http://dx.doi.org/10.1016/j.cherd.2017.01.030

- The continuous replacement of solid sorbent in post-combustion CCS loops is modeled.
- The known method removes/replaces a constant amount of sorbent after each iteration.
- Known method discards fresher material, too, as the looping sorbent is fully mixed.
- We can sort removed CO2-loaded sorbent: the fresher is denser due to higher capacity.
- Our novel strategy puts freshest sorbent back; we compute the reduced need of sorbent.

Selective strategy for solid sorbent replacement in CCS

Giuseppe Colantuono[a,b,*], Timothy Cockerill[a]

[a] *Centre for Integrated Energy Research, School of Chemical and Process Engineering, University of Leeds, LS2 9JT, Leeds, UK*
[b] *School of Built Environment and Engineering, Leeds Beckett University, LS1 3HE, Leeds, UK*

Abstract

An innovative method for sorbent replacement in the looping of a generic solid sorbent for post-combustion carbon capture and sequestration (CCS) is introduced. First, the standard replacement method is revisited with some original results presented. A new strategy is then modeled, aimed at selectively replacing the material as it degrades. This method exploits the density difference, after adsorption, between relatively fresh, CO_2-laden sorbent and relatively degraded material, with small residual adsorption capacity. The model is then applied to values of degradation rate within the experimental range available in scientific literature for silica-supported amines (SSA). The selective removal strategy ideally allows a saving of 37% of the sorbent with respect to the standard, undifferentiated replacement considered in first place, while keeping the same adsorptive capacity of the system.

Keywords: carbon capture loop; solid sorbent; silica-supported amines; capacity degradation; sorbent replacement; make-up flow.

1. Introduction

Novel solid sorbents offer advantages over more established liquid amines for application in next generation carbon dioxide capture plants. In particular, their small thermal mass is expected to produce a more energy efficient capture process, while other physical and chemical properties result in a lower toxicity (Buist et al., 2015; McDonald et al., 2014). The capacity of a solid sorbent to capture carbon dioxide degrades over time with the number of sorption/desorption cycles (cy) endured, and hence there is an on-going need to replace material in order to maintain plant performance. With calcium looping (CaL), the input mass rate of fresh sorbent can be of the same order of magnitude as that of the fuel supply (Hanak et al., 2015); however, low sorbent cost makes replacement less of an obstacle to an economically viable process. Novel solid sorbents can

*Corresponding author, colantuono@gmail.com

be very expensive instead, such that replacement rate has a significant impact on operating costs.

Minimizing the fresh sorbent requirement for next generation CCS plants is therefore vital to make the technology economically viable. The only replacement method considered so far (Abanades, 2002) substitutes a fixed mass of randomly-picked sorbent particles each time a sorption/desorption looping *cy* takes place. While effective in maintaining plant performance, this approach discards both degraded and recently added material from the well-mixed circulating sorbent.

This study investigates a modified strategy in which the sorbent is sorted by density after removal in order to return to the loop the still-active particles, therefore minimizing the unnecessarily replaced material. Replacement occurs after the sorption stage, when the fresher material has a higher density thanks to its higher affinity for carbon dioxide. In principle, this allows only material below a chosen density threshold, corresponding to a particular capacity threshold, to be removed. A mathematical model is developed, to investigate the key characteristics of the replacement process. Replacement rate reduction is computed as function of key sorbent properties and number of *cy* undergone by the system.

The present work has been carried out in support of a program focused on the development of a novel Silica Supported Amine (SSA) adsorbent for CO_2 capture from gas-fired power plants (Liu et al., 2013). However, many kinds of solid adsorbents are under consideration (Wang et al., 2014a; Huck et al., 2014), based on a variety of solid substrates (Kong et al., 2015; Hao et al., 2013; Plaza et al., 2012): the potential application of the analysis is therefore broad.

2. Degradation and replacement rate for solid sorbents

The replacement rate depends on the sorbent rate of loss of adsorption capacity (degradation) per *cy*. Table 1 reports the experimental degradation rates of several silica-supported amines (SSA). Significant dissimilarities exist between testing a solid sorbent in the lab (e.g. Sayari et al., 2012) and conditions in a real plant. Laboratory experiments are usually performed on few kg of sorbent or less, while industrial loops are expected to move many thousands of kg in a continuous process. In the lab, sorbent is often kept in the adsorption mode until CO_2 saturation occurs. The batch then sometimes undergoes the desorption phase in the same location, usually at higher temperature and for a longer time (e.g. Franchi et al., 2005). No study seems to go beyond few tens of *cy*, which is a major knowledge gap as industrial applications are likely to require thousands of *cy*.

When a continuous looping is reported (in Zhao et al., 2013a, sorbent is moved back and forth from an adsorption to a desorption vessel), the number of *cy* is still very small, for a total of some tens of hours: sorbent is not nearly fully degraded. In fact, some materials reported in Table 1 do not display any noticeable degradation: these are probably worth a deeper investigation. Some degradation trends can be hypothesized (Fig. 1) for the more decay-prone

Table 1: The constitutive relationship between age and adsorbing capacity is reported from the experimental studies cited in first column. N, the total number of adsorption/desorption cycles, appears in third column. Most studies are in good agreement with a linear fit of negative slope γ' (column 4) representing the percent drop per cy: $\gamma' = 100\,\gamma$, where γ is the slope in the main text. A few cases show a seemingly nonlinear decay in the initial few cy, followed by an approximate linear trend; such initial nonlinearity is neglected here, as what matters is the behavior in the long run (from 10 to 10^3 cy). BTC stands for "breakthrough capacity" (Zhang et al., 2014b): the adsorption phase is considered achieved once CO_2 concentration in the flue gas flowing out of the adsorption vessel falls to 10% of CO_2 concentration in the input flue gas. Slopes are normalized such that the capacity of fresh sorbent (β in the main text) equals 1. The trends reported in this table are depicted in Fig. 1.

Reference	Sorbent name	N	γ', $\frac{\%}{\text{cy}}$	Notes
(Zhang et al., 2014b)	40% PEI-silica	24	−1.4	dry; BTC
		57	0.0	moist; BTC
(Franchi et al., 2005)	6.98DEA/PE-MCM	7	−0.6	
" "	MCM-41-PEI50	7	−1.0	(Xu et al., 2002)
" "	Zeolite 13X	5	0.0	regene- 350 °C
" "		6	−7.1	rate at: 75 °C
(Zhao et al., 2013a)		10	0.0	dual fluid. beds
(Zhao et al., 2013b)	PEI600-Q10	10	−0.9	
" "	PEI1200-Q10	10	0.0	
" "	PEI800-Q10	10	0.0	
" "	TEPA-Q10	10	0.0	
(Sayari et al., 2012)	pMono-50/130	31	−1.6	dry
" "	sMono-1-50/130	31	0.0	dry
" "	Diamine-50/130	31	−1.8	dry; nonlinear
" "	DiSamine-50/130	31	−1.8	" "
" "	TRI-50/130	31	−1.6	" "
" "	LPEI-50/130	31	−1.5	dry
" "	LPEI-50/150	31	−2.6	dry; nonlinear
" "	BPEI-50/130	31	−1.9	" "
" "	PALL-100/160	31	−0.4	" "

materials, but can be hardly extrapolated beyond a drop in capacity of few percent.

3. Standard replacement method

A looping system for CO_2 capture is here analyzed with regards to the gradual replacement of the solid sorbent to maintain the plant adsorption capacity. The plant (Fig. 2) moves material between two circulating fluidized beds. In the first one, the CO_2-laden flue gas is blown through the sorbent (Zhao et al., 2013a; Rodriguez et al., 2010; Wang et al., 2014c) and CO_2 is adsorbed. In the second bed CO_2 is removed (the sorbent is regenerated), for example by fanning nitrogen (e.g. Zhao et al., 2013a; Drage et al., 2008).

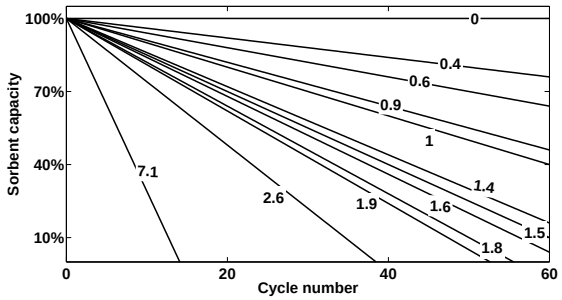

Figure 1: Decay trends from Table 1; labels indicate the slope $|\gamma'| = 100\,|\gamma|$: the loss of adsorption capacity per *cy* of the aging sorbent. Capacity of fresh sorbent is set to 1.

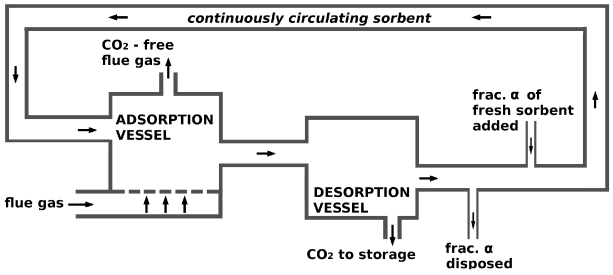

Figure 2: Schematic representation of the CCS loop with standard replacement procedure.

The system starts with a batch of fresh sorbent. After the first cycle, a fraction α is removed (Fig. 2) and replaced with an equivalent amount of fresh material. Before *cy* 2, the sorbent is therefore made up of a fraction $(1-\alpha)$

Table 2: Age distribution in the system after N *cy*; α is the replacement rate. The first column tells the age of the fraction of material reported in column 2 (which sums up to 1, the entirety of material in the system); column 3 indicates the *cy* number at which the respective fraction was introduced in the system.

Age	Fraction of sorbent	Inserted at cycle
$k = 0$	α	$n = N$
$k = 1$	$\alpha(1-\alpha)$	$n = N-1$
$k = 2$	$\alpha(1-\alpha)^2$	$n = -2$
$\vdots$	$\vdots$	$\vdots$
$k = N-1$	$\alpha(1-\alpha)^{N-1}$	$n = 1$
$k = N$	$(1-\alpha)^N$	$n = 0$

of 1-*cy*-old sorbent and a fraction α of fresh sorbent. After *cy* 2, a further fraction α is removed and replaced. The removed material is made up by a fraction $\alpha(1-\alpha)$ of 2-*cy*-old sorbent and a fraction α^2 of 1-*cy*-old sorbent.

Immediately before cy 3, the sorbent therefore consists of a 2-cy-old fraction $(1-\alpha)^2$, a 1-cy-old fraction $\alpha(1-\alpha)$, and in a fraction α of fresh material. In Table 2, the procedure is generalized to an arbitrary number of cy N. Due to the turbulent dynamics of circulating fluidized beds (Grace et al., 2012) it is hypothesized that (Rodriguez et al., 2010; Grasa et al., 2009; Abanades, 2002), for each integer $N>0$, the fresh sorbent introduced right after cy N will be completely mixed as soon as cy $N+1$ is complete. After N cy characterized by a replacement rate α, the amount of material of a given age $k \leq N$ present in the plant is provided by the distribution of ages

$$f(k;\alpha,N) \;=\; \alpha^{1-\delta_{kN}}\,(1-\alpha)^k\,, \tag{1}$$

where

$$\delta_{kN} \;=\; \begin{cases} 1, & \text{if} \quad k=N \\ 0, & \text{otherwise,} \end{cases}$$

is the Kronecker Delta.

The average age of the circulating material is calculated by means of introducing the weighted distribution of ages

$$w(k;\alpha,N) \;=\; k\,\alpha^{1-\delta_{kN}}\,(1-\alpha)^k \tag{2}$$

and then summing from 0 to N:

$$\overline{K}(\alpha,N) \;\equiv\; \sum_{k=0}^{N} w(k;\alpha,N) \;=\; (1-\alpha)\,\frac{1-(1-\alpha)^N}{\alpha}\,. \tag{3}$$

Equation (3) immediately follows from Eq. (2) and the formula for the partial sum of the geometric series (Gradshteyn and Ryzhik, 1980). When the number of cy N approaches infinity, the average age becomes

$$\overline{K}^{\infty}(\alpha) \;\equiv\; \sum_{k=0}^{\infty} w(k;\alpha,\infty) \;=\; \frac{(1-\alpha)}{\alpha} \underset{\alpha\ll 1}{\sim} \frac{1}{\alpha}\,. \tag{4}$$

That is, after a large number of cycles and for a small replacement rate α, the average age of the sorbent in the system is inversely proportional to α. Abanades (2002) carries out a similar analysis (later expanded by Grasa et al. 2009, Rodriguez et al. 2010 and Martínez et al. 2012) for a carbonation-calcination loop and computes the asymptotic value of absorption capacity for an infinite number of cy. Instead, average age is here computed for any finite N; the asymptotic behavior is then obtained. Capacity is introduced at a later stage, as its dependency on age (constitutive relationship) is material dependent.

4. Selective replacement method

Replaced sorbent α for the standard method consists of perfectly mixed ages/capacities, as occurs for the whole system: fresher sorbent is therefore disposed of at the same rate of older material, which is wasteful.

The difference in the mass of sorbent particles before and after adsorption reaches $\sim 14\%$ in some studies (Wang et al., 2014b). According to accepted theories on physical adsorption (Brunauer-Emmett-Teller, or BET, and its precursors and evolutions, see for example Rouquerol et al. 2013), the adsorbed gas gets confined, by the Lennard-Jones potential (Mortimer, 2000), in layers within few Å of the surfaces of the sorbent particles. Numerical simulations in Razmus and Hall (1991) show that the adsorbate's density markedly peaks in the adsorption layers with respect to the surrounding fluid phase; the contribution of those layers to the volume of the porous particles is negligible, which holds even more for chemisorption, in which case the adsorbate is confined within a single layer (Dąbrowski, 2001). That is, the mass increment of particles due to adsorption can be regarded as a density increase only, at least at the pressure (within one order of magnitude of 1 bar) at which CO_2 adsorption takes place (Murata et al., 2002).

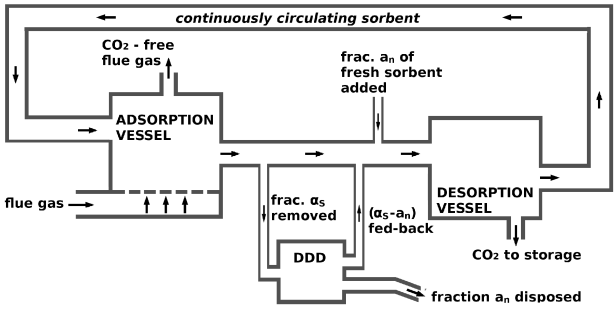

Figure 3: Scheme of the CCS loop proposed for the selective replacement procedure. The density discriminating device (*DDD*) is the novelty with respect to Fig. 2. Replacement is here posited to occur when the sorbent is loaded with CO_2, as the mass gained during absorption allows to discriminate between fresh and degraded material.

Gas-solid fluidized beds are of interest as potential *DDD*'s; it is proposed to use the CO_2 - laden flue gas as the fluidizing medium, in order not to accidentally remove from the sorbent the CO_2 load, and the density difference with it. Denser material will then be reinserted into the looping system, upstream of the desorption vessel, ready for the desorption stage (Fig. 3). In order not to disperse CO_2 in the atmosphere an extra stage is introduced, where the removed degraded material is regenerated prior to its disposal.

4.1. Possible ways to achieve density separation

Density/gravity dry separation methods are subject to intense R&D efforts, driven by the need for burning cleaner coal to reduce pollution (e.g. Xia et al., 2015) and to advance mineral processing, waste recycling and other industries. Additional techniques are combined with fluidization to improve separation. Air dense medium fluidized beds (ADMFBs, Mohanta et al. 2013) have existed for almost a century (Fraser and Yancey, 1925). They work by mixing a "separation medium" (usually a finer powder than the one being sorted) with air to obtain

the fluidizing medium, the density of which is tuned to the wanted separation density. Separation is ideally achieved relying on buoyancy only, like in a liquid. Turbulence due to bubble formation induces vertical mixing, thus working against density stratification and separation (Mohanta et al., 2013). Vibration is often applied to ADMFBs to reduce bubble size and mixing (Luo et al., 2003); stabilization can be intensified also by using a magnetizable separation medium and applying a magnetic field (Luo et al., 2002).

Many studies report separation of particles with diameter down to half millimeter (see references in Mohanta et al., 2013, who also point out the current drawbacks of the method and the need of further development). Luo et al. (2002) employ magnetic pearls and achieve segregation of coal particles between 0.5 mm and 6 mm, the separation density being $\rho_0 = 1520\,\mathrm{kg\,m^{-3}}$, with an Ecart probable error

$$E_p \equiv (\rho_{75} - \rho_{25})/2 = 65\,\mathrm{kg\,m^{-3}} \tag{5}$$

(values $\rho_{25} < \rho_0 < \rho_{75}$ are defined such that the denser fraction after separation "erroneously" contains 25% of ρ_{25}-dense sorbent and "only" 75% of the denser-than-threshold material ρ_{75}. Particles with density within/outside the $[\rho_{25}, \rho_{75}]$ interval are harder/easier to separate, Richard et al. 2011).

Choung et al. (2006) focus on the submillimiter range (0.4 to 1.0 mm) and attain separation with $E_p = 100\,\mathrm{kg\,m^{-3}}$ using an ADMFB. Tenths of mm is also the typical size of SSA particles for carbon capture reported in some characterization studies reviewed in Table 1 (e.g. Zhang et al., 2014b). Sahan and Kozanoglu (1997) employ a magnetized ADMFB to separate fines down to few tens of µm, grouping particles by size prior to the separation process (e.g., 45 to 75 µm): this way, drag forces (acting on particles in proportion to their size) are comparable, and affect less the buoyancy discriminating effect. E_p is not reported, but their work is relevant as SSA particles for CCS can be manufactured to display a narrow size distribution (Zhao et al., 2013a) which helps density sorting.

4.2. Consequence of separation errors

The density range $2E_p$ (Eq. 5) for the just reported studies is comparable to the ~ 200 kg/m^3 estimated difference between fresh- and worn-out- post-adsorption SSA (based on the adsorption capacity of 142 mg of CO_2 per g of sorbent, reported by Wang et al. 2014b, multiplied by the 1400 kg/m^3 SSA density of Zhang et al. 2014a). Some degree of separation could already be possible, at least between freshest and oldest SSA particles; development of sorbents with higher adsorption capacity will increase density difference between fresh and spent sorbent, making separation sharper.

Aside from the separation technique it is necessary to estimate the outcome of mistakenly categorizing a particle of density $\rho_0 - \epsilon\rho_0$ as having density $\rho_0 + \epsilon\rho_0$ (with $\epsilon < 1$) while, on the other side, labeling a $\rho_0 + \epsilon\rho_0$ particle as a $\rho_0 - \epsilon\rho_0$ one. If $\epsilon \ll 1$, the *DDD* gets rid of a particle of capacity slightly higher than the retained particle. Highly probable small errors have therefore small impact. The errors with notable effects (e.g. exchanging a particle with 80%

capacity with one of 20%) are the least probable instead. Such an advantageous inverse relationship between sorting errors magnitude and the likelihood of their occurrence is not found in the cited studies about density separation devices. Density sorting is there employed as a binary classifier, to filter out impurities in coal or other materials. A separation error in those contexts has always the maximal outcome: retaining the wrong species in place of the desired one, no matter how small the density difference is. Viceversa, the process outlined here will be practically unaffected by separation errors at small density differences, and may still be worthwhile in presence of large separation errors.

As a simple measure of the effectiveness of a coarse separation, a set of 101 pairs of CO_2-loaded particles is considered; each pair is labeled from 0 to 100 to indicate age n. A density-separation process is then performed, with the aim of obtaining two sets of 101 particles each. In case of perfect separation, set A contains the older/lighter particles (50 pairs from age 51 to age 100, plus one particle of age 50), whilst set B contains the fresher/denser particles (50 particle pairs from age 0 to age 49, plus one particle of age 50); the sum of ages is 7550 for set A and 2550 for set B. In case of separation able to discriminate only particles with $n \geq 90$ from particles with $n \leq 10$ (i.e. density difference $160\,\mathrm{kg\,m^{-3}}$ or larger, being $200\,\mathrm{kg\,m^{-3}}$ the difference between fresh and completely worn-out sorbent estimated few lines above), the age sum is 6040 for set A and 4060 for set B, meaning that 40% of the adsorption capacity imbalance in the system can be discriminated. In case of a $120\,\mathrm{kg\,m^{-3}}$ *DDD*'s resolution limit (i.e., the *DDD* is able to discriminate only particles with $n \geq 80$ from particles with $n \leq 20$), 70% of sorption capacity difference can be separated. This simple estimate shows how the *DDD* can be far from ideal but still useful.

Fines may form in the capture plant due to particles crumbling; this occurs almost only in the first few cycles. On the other hand, smaller particles tend to agglomerate as *cy* number increases (Fig. 3 in Zhang et al., 2014b). This reduces the spread of the particles' size distribution, therefore helping the sharpness of *DDD* separation.

5. Mathematical model of the selective replacement

The amount of make-up sorbent needed in a loop with a *DDD* is determined and compared with the larger quantity needed in the standard case. The *DDD* operates with a density threshold reached by the progressively degraded CO_2 -loaded sorbent after M *cy*. During the initial $M-1$ *cy*, no material is removed. Right after *cy* M, a predetermined fraction α_S is taken away and replaced with fresh sorbent (age 0). After *cy* $M+1$ a further fraction α_S is removed; this amount is not homogeneous, because the plant contains the fraction $(1-\alpha_S)$ of original sorbent (now aged $M+1$), plus the fraction α_S of sorbent inserted at the end of the previous *cy*. We adopt the "ket" notation $|\,\rangle$ to indicate the *cy* number at which the sorbent was inserted as fresh, and therefore label with $|M\rangle$ the material inserted right after *cy* M. The expression $(1-\alpha_S)\,|0\rangle$ denotes the amount of the oldest material that is still present in the system right after *cy* M and the following replacement procedure has been accomplished. As

a consequence, the fraction α_S removed after *cy* $M+1$ has two components: $\alpha_S(1-\alpha_S)\,|0\rangle$ and $\alpha_S^2\,|M\rangle$. The hypothesis that all the ages in the plant are completely mixed holds also for selective replacement.

The *DDD* outlined above now starts to operate: the component $\alpha_S^2\,|M\rangle$ can be separated from the older, lighter component $\alpha_S(1-\alpha_S)\,|0\rangle$, and returned to the looping system. The net effect of the replacement procedure is to substitute $\alpha_S(1-\alpha_S)\,|0\rangle$ with $\alpha_S(1-\alpha_S)\,|M+1\rangle$. The composition of the sorbent ready for *cy* $M+2$ is therefore $(1-\alpha_S)^2\,|0\rangle+\alpha_S\,|M\rangle+\alpha_S(1-\alpha_S)\,|M+1\rangle$.

The fraction removed after *cy* $M+2$ is then $\alpha_S\cdot[(1-\alpha_S)^2\,|0\rangle+\alpha_S\,|M\rangle+\alpha_S(1-\alpha_S)\,|M+1\rangle]$; the last two terms are fed-back into the desorption vessel, implying that the truly disposed-of material is only $\alpha_S(1-\alpha_S)^2\,|0\rangle$, replaced by $\alpha_S(1-\alpha_S)^2\,|M+2\rangle$. The difference with the standard procedure (Abanades, 2002) resides in putting back into the system the sorbent that is less than M *cy* old.

In order to derive a general expression for the replacement, the following procedure is formulated for an arbitrary number of *cy* N, with M denoting the age threshold (the number of *cy* needed to degrade the material). The sorbent in the system is divided in three categories: the fraction of material present from the outset, labeled by $|0\rangle$; the fractions introduced after *cy* M and before N–M, labeled by $|M\rangle, |M+1\rangle, |M+2\rangle, ..., |N-M\rangle$; and the fractions of sorbent less than M-*cy* old, labeled by the highest *cy* numbers, from $|N-M+1\rangle$ to $|N\rangle$. The material designated by the highest labels is the one that the *DDD* puts back into the desorption vessel, as schematized in Fig. 3. The age distribution of the sorbent, after the replacement occurring between *cy* N and $N+1$, is

$$|S_{N,M}\rangle = |0\rangle\,, \qquad \text{if} \quad N < M \tag{6}$$

$$|S_{N,M}\rangle = (1-\alpha_S)^{N-M+1}\,|0\rangle + \sum_{n=M}^{N-M} a_n\,(1-\alpha_S)^{N-M-n+1}\,|n\rangle + \\ + \sum_{n=N-M+1}^{N} H(n-M+1)\;a_n\,|n\rangle\,, \qquad \text{if} \quad N \geq M\,; \tag{7}$$

the summations (for Eq. 7 and all the following ones) are nil if the upper limit is smaller than the lower one. The quantity

$$H(X) = \begin{cases} 1, & \text{if } X > 0\,; \\ 0, & \text{otherwise} \end{cases} \tag{8}$$

is the Heaviside step function according to the $H(0)=0$ convention, while the coefficients $0 \leq a_n \leq 1$ in Eq. (7) are unknown ad need to be determined. The a_n's represent the replacement rate at *cy* n, as shown in Fig. 4: the fraction α_S is picked and processed by the *DDD*; the fraction a_n (the "oldest" subset of α_S) is replaced with fresh sorbent, and the fraction $\alpha_S - a_n$ is put back in the system. a_n varies with the *cy* number, but gradually approaches its asymptotic value a_∞. The norm (a.k.a. the modulus for ordinary vectors) of

$|S_{N,M}\rangle$ (Eq. 7) is equal to 1, as $|S_{N,M}\rangle$ is the sum of all the components in the system.

The case $N < M$ (Eq. 6) can be neglected, as it corresponds to ending the loop before the threshold age is reached. By multiplying each $|n\rangle$ by the age $k = N - n$ in Eq. (7), the sorbent average age is computed, in analogy with Eq. (3):

$$\overline{K}_S = N\,(1-\alpha_S)^{N-M+1} + \sum_{n=M}^{N-M} a_n\,(N-n)\,(1-\alpha_S)^{N-M-n+1} + \\ + \sum_{n=N-M+1}^{N} H(n-M+1)\;(N-n)\;a_n\,. \tag{9}$$

Starting from Eq. (7) we now define

$$|S^M_{N,M}\rangle = |S_{N,M}\rangle - \sum_{n=N-M+1}^{N} H(n-M+1)\;a_n\,|n\rangle \equiv \\ \equiv (1-\alpha_S)^{N-M+1}\,|0\rangle + \sum_{n=M}^{N-M} a_n\,(1-\alpha_S)^{N-M-n+1}\,|n\rangle\,, \tag{10}$$

the portion of sorbent in the system that has already crossed the threshold M, and from which the removed sorbent must be drawn. The amount of material replaced by fresh matter after each *cy* $l = 0, 1, 2, ..., N-1$ is therefore the following fraction of $|S^M_{l,M}\rangle$:

$$a_0 = 1 \tag{11}$$

$$a_1 = a_2 = ... = a_{M-2} = a_{M-1} = 0 \tag{12}$$

$$a_M = \alpha_S\,a_0 \equiv \alpha_S \tag{13}$$

$$\vdots$$

$$a_{l+1} = \alpha_S\,\left\|S^M_{l,M}\right\| \equiv \\ \equiv \alpha_S\left[a_0\,(1-\alpha_S)^{l-M+1} + \sum_{n=M}^{l-M+1} a_n\,(1-\alpha_S)^{l-M-n+1}\right]. \tag{14}$$

The material $a_{l+1}\,|l{+}1\rangle$, inserted right after *cy* $l{+}1$, starts to be removed after *cy* $l{+}M{+}1$. The quantity of sorbent labeled by $|l+1\rangle$, which is still present in the system right after *cy* $l{+}M{+}p \le N$, amounts to $a_{l+1}(1{-}\alpha_S)^p$; p is a positive integer.

The $\{a_n\}$ sequence represents the actual replacement rate of the selective method (Fig. 4-A, dashed curve), and varies with the *cy* number n. The difference between the "nominal", constant replacement rate α_S, and the actual rate, a_n, represents the sorbent above the density threshold, which is returned into the system just before *cy* $n{+}1$.

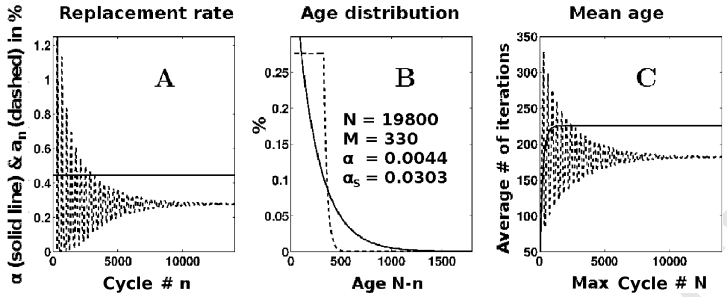

Figure 4: Panel A: the standard procedure for sorbent replacement (constant rate $\alpha \approx 0.44\%$) is compared to the selective strategy (dashed line; nominal replacement rate $\alpha_S \approx 3.03\%$, corresponding to the out-of-box maximum of the curve at $n = M$). The total number of *cy* is N, while M indicates the age threshold for the selective case; that is, the number of *cy* after which the sorbent can be disposed of. Age is proportional to sorbent's capacity (Table 1); hence, to the density of the CO_2-loaded particles. The difference between the asymptotic value $a_\infty \approx 0.28\%$ of the selective method and the standard method's $\alpha \approx 0.44\%$ implies that 37% of sorbent can be saved by the selective procedure. Panel B shows the distribution of ages in the system. Panel C reports the average age of the sorbent in the system as function of the number of elapsed *cy*. The parameters shown in Panel B are common to all the three plots. *The α and α_S rates have been chosen to be in a proportion such that the ensuing age distribution in the system leads to the same asymptotic capacity in both cases (Fig. 5A).*

Equations (11-14) define the sought recursive formula: a_{l+1}, the amount of material to be replaced after *cy* $l+1$, is a linear combination of $|0\rangle$ and of the preceding replacements $|M\rangle, ..., |l-M\rangle$: that is, all and only the labels older than M *cy*. Equation (11) holds because $|0\rangle$ is the label of the sorbent that completely fills the system up before *cy* 1. Equations (12) reflect the fact that, before the initial load of sorbent reaches the threshold age M, no replacement occurs. The first replacement occurs right after *cy* M, when a fraction α_S is removed (Eq. 13). As time and cycle number advance, as soon as any sorbent label $|n\rangle$ becomes M *cy* old, it starts to be depleted by a factor $(1-\alpha_S)$ per *cy*. E.g., right after *cy* 200, only $\sim 21\%$ of the fraction inserted at *cy* 100, a_{100}, is present in the system, as $(1-\alpha_S)^{200-M-100+1} \equiv (1-\alpha_S)^{51} = 0.212$, for $M = 50$ and $\alpha_S = 3\%$.

6. Constitutive relationship between capacity and age

Adsorption capacity can be related to the number of endured adsorption/desorption cycles ("age") using the experimental results cited in Table 1; in most cases, capacity (column 4) fits a linearly decreasing trend with respect to *cy* number. A significant exception is LPEI-50/150 in Sayari et al. (2012), which resembles a negative exponential. Such a shape may be realistic for other materials as well: as soon as tests will last enough to bring capacity closer to zero, a horizontal asymptotic may be expected. Here, decreasing linear trends are adopted (Fig. 1); capacity is then set to zero for every *cy* number greater than the abscissa intercept, in order to avoid non-physical negative values; this choice

makes the constitutive relationship piecewise linear:

$$C(k) \;=\; (\gamma k \;+\; \beta)\cdot H(\gamma k \;+\; \beta)\,, \qquad \gamma \le 0\,, \quad \beta \ge 0\,; \tag{15}$$

the ordinate intercept β is the capacity of fresh sorbent, set to 1 in the numerical experiments (Figs. 4-6) and in Fig 1.

6.1. System's adsorption capacity with standard replacement

The distribution of ages in the system is known (Eq. 1); recalling that Eq. (2) was obtained by weighting the age distribution by the age itself, we now use as weight the capacity $C(k)$ introduced in Eq. (15). The distribution of capacities in the system will then be

$$c(k;\alpha,N) \;=\; (\gamma k \;+\; \beta)\cdot H(\gamma k \;+\; \beta)\;\alpha^{1-\delta_{kN}}\,(1-\alpha)^{k}\,. \tag{16}$$

Consequently, the average capacity is

$$\overline{C}(\alpha,N) \;=\; \sum_{k=0}^{N}(\gamma k \;+\; \beta)\cdot H(\gamma k \;+\; \beta)\;\alpha^{1-\delta_{kN}}\,(1-\alpha)^{k}\,. \tag{17}$$

6.2. System's adsorption capacity with selective replacement

In the selective case, too, the average capacity can be expressed starting from average age (Eq. 9) with capacity $C(k)$ (Eq. 15) playing the role of the weighting function in lieu of age $k \equiv N-n$:

$$\overline{C}_S \;=\; C(N)\,(1-\alpha_S)^{N-M+1} \;+\; \sum_{n=M}^{N-M} a_n\,C(N-n)\,(1-\alpha_S)^{N-M-n+1} \;+$$
$$+\;\sum_{n=N-M+1}^{N} H(n-M+1)\;C(N-n)\;a_n\,. \tag{18}$$

Average capacity $\overline{C}_S$ therefore relies on the recursion formulas for the actual replacement rate a_n (Eqs. 11-14), which are determined numerically (Figs. 5, 6D).

7. How do the two replacement strategies compare?

To compare the sorbent requirement of the selective method against the standard one, we ask for the asymptotic value of the average capacity for large N to be the same in both cases (Fig. 5A). This is accomplished by fixing the nominal replacement rate α_S of the selective case (dashed line) to $\sim$6.87 times the standard replacement rate α (Fig. 4A), and leads (Fig. 4C) to a lower average age with respect to the standard system (solid line), as the older-than-threshold sorbent is selectively, more effectively removed. Such a lower average age does not translate into higher capacity however, because old-enough sorbent has zero capacity regardless of age.

The ratio α_S/α causing the asymptotic matching is controlled by the decay rate γ, as shown in Fig. 5: with γ as in Fig. 5A, the asymptotic value of the selective replacement case (dashed line) is equal to the standard case (solid line). Keeping α_S and α unchanged for a more resilient sorbent (Fig. 5B-C, smaller $|\gamma|$) causes the asymptotic mismatch instead. Even more important, unwanted replacement and disposal of still-fresh sorbent occur both in the standard and selective case, as shown by the higher capacity of the system (∼0.8-0.9 vs 0.5). In order to keep the average capacity constant while increasing resilience (that is, while decreasing $|\gamma|$) α_S and α need to be reduced accordingly, as shown in Fig. 6.

Having set the replacement rates α and α_S as in Fig. 4, Fig. 5 displays the ensuing behavior of capacity as function of the degradation rate γ, which has been fixed to a range of values inversely proportional to the threshold M: $-0.9/M$, $-0.3/M$, and $-0.09/M$. In Fig. 5A (and Fig. 6D), the standard decay rate coincides with the asymptotic value of the selective replacement's capacity, that oscillates around the mean value with the oscillations amplitude decreasing as progressive *cy* number increases.

In a real power plant the initial capacity oscillations need to be damped, in order to suppress/smooth out the few first, very low relative minima (indicating insufficient capture). This could be accomplished for example by starting with a prescribed distribution of ages rather than with a batch of fresh sorbent. Starting capture operations with a distribution of ages approximating the one shown in Fig. 4B for $N = 19800$ (dashed curve, selective procedure) places the system in an operational mode close to the capacity asymptote $\overline{C}_S = 0.5$ shown in Fig. 5A. Approximating initially such a distribution would be relatively easy, as all the ages above $1/|\gamma| \approx 370$ *cy* are equivalent for the sake of both CO_2 capacity (nil) and density separation.

The parameters M, α_S, and γ in Figs. 5A and 6D have been selected in order to exploit the sorbent at least down to 10% of its fresh capacity. Below this threshold value, the sorbent becomes disposable. This does not mean it will be disposed of immediately after crossing the threshold, as the *DDD*, each time, processes a randomly-picked fraction of the circulating sorbent. Figs. 5B-5C summarize the (impractical) configuration in which the chosen threshold M and the replacement rates α and α_S make a more (with respect to Fig. 5A) resilient sorbent disposable at ∼80-95% of full capacity. M, α, and α_S should be modified accordingly in order to compensate for the reduced $|\gamma|$ to obtain a situation similar to Fig. 5A, with an average capacity around 50%, an almost complete exploitation of the sorbent and a consequent detectable density difference between fresh and disposable sorbent: this is attained in Fig. 6D.

On the other hand, increasing the threshold in Fig. 5A to $M = -1/\gamma = 370$ in order to exploit capacity entirely would require $\sim 50\%$ more sorbent being processed by the *DDD*, consequently making the *DDD* larger and costlier. The choice of the parameters is therefore intertwined with the economic equilibrium between the plant components, the sorbent cost and the *DDD* separation effectiveness, and will be addressed in an ongoing study on techno-economics (e.g. Hurst et al., 2012; Odeh and Cockerill, 2008a,b) and uncertainty analysis

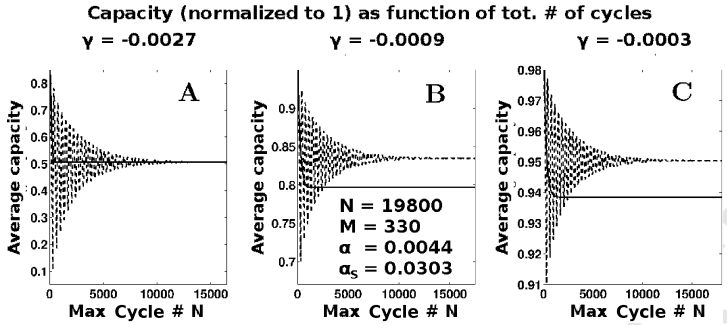

Figure 5: Normalized capacity (ratio of average capacity to the capacity of fresh sorbent) as function of the total number of *cy* N, for both the standard case (after Eq. 17 with $\beta = 1$; solid line) and the selective procedure (Eq. 18; dashed line). Three values for the constitutive relation's slope are considered here, falling within the range of the γ values displayed in Table 1 (spanning from ~ -0.07 to ~ 0; the latter value corresponds to undetectable degradation in the small number of reported cycles). The value of the degradation rate γ of Panel A is divided by 3 in Panel B and by 10 in Panel C. The normalized average capacity values $\overline{C}$, $\overline{C}_S$ shown in these plots correspond to the average age values $\overline{K}$, $\overline{K}_S$ displayed in Fig. 4C. The parameters shown in Panel B are common to all the three plots and to Fig. 4.

of SSA-based CO_2 capture.

Figure 6A-C represent the evolution of Fig. 4A-C, respectively, for a tenfold increase of the threshold M, the according tenfold growth of the number of total *cy* N, and a tenfold reduction of the α, α_S, and a_n rates. Such combined parameters' change has the effect of rescaling the axes while keeping Fig. 6A-C perfectly similar to Fig. 4A-C. Figure 6D, the evolution of Fig. 5A, shows that capacity is left unaltered if the above change in parameters' values is combined with a tenfold reduction of $|\gamma|$. The magnitude of the make-up flow of fresh sorbent therefore critically depends on sorbent's resilience, quantified by the slope γ in the hypothesis of a linear age-capacity constitutive relationship.

Selective actual replacement rate (Fig. 4A, dashed line) and average age (Fig. 4C) settle reasonably close to their asymptotic values after a number of *cy* less than $10M$ (which is the value of N used in the numerical computations summarized in Figs. 4, 5 and 6). The age distribution, too (Fig. 4B), is insensitive to increasing N beyond $\sim 10M$: the sorbent labels (ages) present in the system in significant amounts are the ones inserted in the most recent cycles, regardless to the overall length of the process.

Mathematically proving the convergence of the series defined by Eqs. (11-14) is not the aim of the present work. To ensure convergence for any practical purpose, a simulation has been run with the same parameters specified in Fig. 4: $\alpha = 3 \cdot 10^{-3}$, $\alpha_S = 4.2 \cdot 10^{-3}$, $M = 330$, but the total number of *cy* increased to $N = 3.3 \cdot 10^5$. With a single complete *cy* taking ~ 2 hr, as reported for example by Zhang et al. (2014b), the corresponding time span is ~ 75 years. The empirical asymptotic value $a_\infty \approx 2.8 \cdot 10^{-3}$ for the selective case (Fig. 4A) is confirmed also on this timescale, with fluctuations around the true value in the order of 10^{-15}.

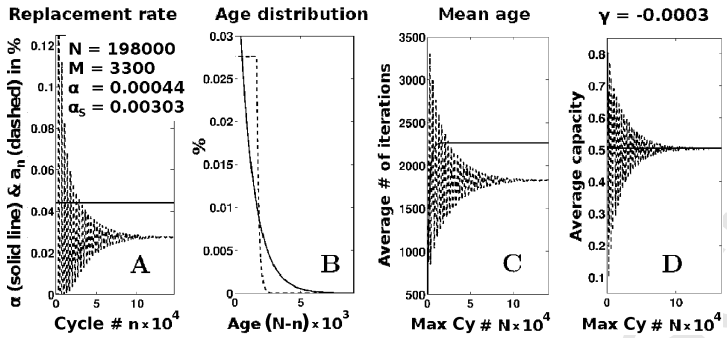

Figure 6: Panels A-C are like Fig. 4A-C but with a tenfold increase of threshold M and number of total cy N, and a tenfold decrease of α, α_S, and a_n ; the parameters shown in Panel A are common to all the four plots. Panel D is similar to Fig. 5A: normalized capacity remains unaltered if, besides the above parameters' changes, $|\gamma|$ is reduced by a factor 10.

The selective replacement strategy simulated as reported in Fig 4, Fig 5A, and Fig 6 allows to save ideally $\sim$37% of sorbent with respect to the standard strategy. A real *DDD* will have this figure modulated by separation efficiency, a simple "worst-case" estimate of which has been provided at the bottom of Section 4.1.

8. Conclusions and recommendations

A key challenge for many types of post-combustion CCS plants is to maintain the effectiveness of the carbon-dioxide capturing sorbent as the plant operates over the long term. With the current interest in solid sorbents, identifying strategies to maintain plant performance is an important topic, that has not been thoroughly covered in the literature.

Most work to date has investigated schemes whereby a constant fraction of the sorbent material is replaced from the plant each time it iterates through the absorption/desorption cycles. As the sorbent particles are well mixed, this approach has the disadvantage that both recently added, relatively-fresh particles will be replaced as well as much older, degraded material.

Building on the work of Abanades (2002), we have analyzed the continuous partial replacement of solid sorbent in a post-combustion CCS adsorption/desorption loop . Analytical expressions have been developed for the distribution of the sorbent particles age and the corresponding adsorption capacity as a function of the number of adsorption/desorption cycles carried out. This analysis allows the potential benefits of a novel strategy for sorbent replacement, exploiting the decrease of adsorption capacity with sorbent age, to be thoroughly modeled and evaluated.

The novel strategy is initially similar to the previously analyzed standard replacement method: a constant fraction of sorbent is removed from the plant with each cycle of the absorption/desorption loop. The innovation proposed here is that the removed particles are subsequently sorted by density. The

reduced capture capacity of the older particles means that, after the adsorption stage, they will have a lower density than the fresher material. As it has been demonstrated that the adsorption process has no impact on particle volume, grading by density is therefore equivalent to grading by capture capacity, and hence particle age. The older fraction of the separated sorbent can then be replaced with fresh material, and the newer fraction returned to the plant, thereby minimizing the need for new sorbent.

Results indicate that, under optimal separation, there would be a 37% make-up flow reduction compared to the strategy without density separation. This figure depends on the separation efficiency. Whether the *DDD* approach is worthwhile depends in principle also on the sorbent's cost and degradation rate γ, as well as on the expenditure on the separation apparatus. The cost the *DDD* adds to generated power scales with the *DDD* size and therefore with the amount of material per *cy* in need of density sorting, which is proportional to γ. The techno-economics of selective replacement will be the subject of a follow-up paper. For a relevant portion of pairs of sorbent's cost and degradation rate values, initial analysis indicates that the *DDD* outlay is much smaller than the expense on material the *DDD* prevents; the overall savings are therefore significant.

The device to accomplish density separation could be an adaptation/evolution of Air Dense Medium Fluidized Beds. ADMFBs use fines in addition to air as the fluidizing medium, which is therefore characterized by a tunable density, to be fixed to the separation threshold: this allows buoyancy-driven separation like in liquids. Separation can be aided by vibration, magnetization, and by a narrow distribution of particles' size. ADMFBs, currently subjects of active development, need to be envisioned as part of a CCS looping system to model and implement the necessary updates to their functioning modes. The increase of sorbent adsorption capacity will also improve separation.

Regardless to replacement strategy, industrial implementation of solid sorbents CO_2 capture needs much longer material characterization tests than the ones currently available, which are limited to few tens of cycles. Thousands of cycles will be necessary in order to explore sorbent degradation, presently unknown beyond a few percent drop from fresh capacity for the most degradation-prone materials, and completely unknown for the most resilient ones.

9. Acknowledgments

The authors are thankful to Prof. Z. Xiao Guo, University College London, and to Profs. Colin Snape and Hao Liu, University of Nottingham, for useful suggestions and discussions. This work was supported by EPSRC Research Grant EP/J020745/1.

References

Abanades, J. C. (2002). The maximum capture efficiency of CO_2 using a carbonation/calcination cycle of $CaO/CaCO_3$. *Chemical Engineering Journal*, 90:303–306.

Buist, H., Devito, S., Goldbohm, R., Stierum, R., Venhorst, J., and Kroese, E. (2015). Hazard assessment of nitrosamine and nitramine by-products of amine-based ccs: Alternative approaches. *Regulatory Toxicology and Pharmacology*, 71(3):601–623.

Choung, J., Mak, C., and Xu, Z. (2006). Fine coal beneficiation using an air dense medium fluidized bed. *Coal Preparation*, 26(1):1–15.

Dąbrowski, A. (2001). Adsorption – from theory to practice. *Advances in colloid and interface science*, 93(1):135–224.

Drage, T., Arenillas, A., Smith, K., and Snape, C. (2008). Thermal stability of polyethylenimine based carbon dioxide adsorbents and its influence on selection of regeneration strategies. *Microporous and Mesoporous Materials*, 116:504 – 512.

Franchi, R. S., Harlick, P. J., and Sayari, A. (2005). Applications of pore-expanded mesoporous silica. 2. development of a high-capacity, water-tolerant adsorbent for CO_2. *Industrial & Engineering Chemistry Research*, 44(21):8007–8013.

Fraser, T. and Yancey, H. F. (1925). The air sand process of cleaning coal. US Patent U.S. Patent No. 1534846.

Grace, J. R., Knowlton, T., and Avidan, A. (2012). *Circulating fluidized beds*. Springer Science & Business Media.

Gradshteyn, I. and Ryzhik, I. (1980). Table of integrals, series, and products: corrected and enlarged edition.

Grasa, G., Abanades, J. C., and Anthony, E. J. (2009). Effect of partial carbonation on the cyclic cao carbonation reaction. *Industrial & Engineering Chemistry Research*, 48(20):9090–9096.

Hanak, D. P., Anthony, E. J., and Manovic, V. (2015). A review of developments in pilot-plant testing and modelling of calcium looping process for CO_2 capture from power generation systems. *Energy & Environmental Science*, 8(8):2199–2249.

Hao, W., Björkman, E., Lilliestråle, M., and Hedin, N. (2013). Activated carbons prepared from hydrothermally carbonized waste biomass used as adsorbents for CO_2. *Applied Energy*, 112:526–532.

Huck, J. M., Lin, L.-C., Berger, A. H., Shahrak, M. N., Martin, R. L., Bhown, A. S., Haranczyk, M., Reuter, K., and Smit, B. (2014). Evaluating different classes of porous materials for carbon capture. *Energy & Environmental Science*, 7(12):4132–4146.

Hurst, T. F., Cockerill, T. T., and Florin, N. H. (2012). Life cycle greenhouse gas assessment of a coal-fired power station with calcium looping CO_2 capture and offshore geological storage. *Energy & Environmental Science*, 5(5):7132–7150.

Kong, Y., Shen, X., Cui, S., and Fan, M. (2015). Development of monolithic adsorbent via polymeric sol–gel process for low-concentration CO_2 capture. *Applied Energy*, 147:308–317.

Liu, H., Guo, Z., Sun, C., Drage, T., Snape, C., and TT, C. (2013). Establishing Solids Looping as a Next Generation NG PCC Technology; EPSRC Project. GrantRef=EP/J020745/1. Abstract available at: http://gow.epsrc.ac.uk/NGBOViewGrant.aspx?

Luo, Z., Zhao, Y., Chen, Q., Fan, M., and Tao, X. (2002). Separation characteristics for fine coal of the magnetically fluidized bed. *Fuel Processing Technology*, 79(1):63–69.

Luo, Z., Zhao, Y., Tao, X., Fan, M., Chen, Q., and Wei, L. (2003). Progress in dry coal cleaning using air-dense medium fluidized beds. *Coal Preparation*, 23(1-2):13–20.

Martínez, A., Lara, Y., Lisbona, P., and Romeo, L. M. (2012). Energy penalty reduction in the calcium looping cycle. *International Journal of Greenhouse Gas Control*, 7:74–81.

McDonald, J. D., Kracko, D., Doyle-Eisele, M., Garner, C. E., Wegerski, C., Senft, A., Knipping, E., Shaw, S., and Rohr, A. (2014). Carbon capture and sequestration: an exploratory inhalation toxicity assessment of amine-trapping solvents and their degradation products. *Environmental science & technology*, 48(18):10821–10828.

Mohanta, S., Rao, C., Daram, A., Chakraborty, S., and Meikap, B. (2013). Air dense medium fluidized bed for dry beneficiation of coal: technological challenges for future. *Particulate Science and Technology*, 31(1):16–27.

Mortimer, R. G. (2000). *Physical Chemistry (Second Edition)*. Academic Press.

Murata, K., Miyawaki, J., and Kaneko, K. (2002). A simple determination method of the absolute adsorbed amount for high pressure gas adsorption. *Carbon*, 40(3):425–428.

Odeh, N. A. and Cockerill, T. T. (2008a). Life cycle analysis of uk coal fired power plants. *Energy conversion and management*, 49(2):212–220.

Odeh, N. A. and Cockerill, T. T. (2008b). Life cycle ghg assessment of fossil fuel power plants with carbon capture and storage. *Energy Policy*, 36(1):367–380.

Plaza, M., González, A., Pevida, C., Pis, J., and Rubiera, F. (2012). Valorisation of spent coffee grounds as CO_2 adsorbents for postcombustion capture applications. *Applied Energy*, 99:272–279.

Razmus, D. M. and Hall, C. K. (1991). Prediction of gas adsorption in 5a zeolites using monte carlo simulation. *AIChE journal*, 37(5):769–779.

Richard, G. M., Mario, M., Javier, T., and Susana, T. (2011). Optimization of the recovery of plastics for recycling by density media separation cyclones. *Resources, Conservation and Recycling*, 55(4):472–482.

Rodriguez, N., Alonso, M., and Abanades, J. (2010). Average activity of cao particles in a calcium looping system. *Chemical Engineering Journal*, 156(2):388 – 394.

Rouquerol, J., Rouquerol, F., Llewellyn, P., Maurin, G., and Sing, K. S. (2013). *Adsorption by powders and porous solids: principles, methodology and applications*. Academic press.

Sahan, R. and Kozanoglu, B. (1997). Use of an air fluidized bed separator in a dry coal cleaning process. *Energy conversion and management*, 38(3):269–286.

Sayari, A., Heydari-Gorji, A., and Yang, Y. (2012). CO_2-induced degradation of amine-containing adsorbents: reaction products and pathways. *Journal of the American Chemical Society*, 134(33):13834–13842.

Wang, J., Huang, L., Yang, R., Zhang, Z., Wu, J., Gao, Y., Wang, Q., O'Hare, D., and Zhong, Z. (2014a). Recent advances in solid sorbents for co 2 capture and new development trends. *Energy & Environmental Science*, 7(11):3478–3518.

Wang, W., Xiao, J., Wei, X., Ding, J., Wang, X., and Song, C. (2014b). Development of a new clay supported polyethylenimine composite for co 2 capture. *Applied Energy*, 113:334–341.

Wang, W., Xiao, J., Wei, X., Ding, J., Wang, X., and Song, C. (2014c). Development of a new clay supported polyethylenimine composite for CO_2 capture. *Applied Energy*, 113(0):334 – 341.

Xia, W., Xie, G., and Peng, Y. (2015). Recent advances in beneficiation for low rank coals. *Powder Technology*, 277:206–221.

Xu, X., Song, C., Andresen, J. M., Miller, B. G., and Scaroni, A. W. (2002). Novel polyethylenimine-modified mesoporous molecular sieve of mcm-41 type as high-capacity adsorbent for CO_2 capture. *Energy & Fuels*, 16(6):1463–1469.

Zhang, W., Liu, H., Sun, C., Drage, T. C., and Snape, C. E. (2014a). Capturing co 2 from ambient air using a polyethyleneimine–silica adsorbent in fluidized beds. *Chemical Engineering Science*, 116:306–316.

Zhang, W., Liu, H., Sun, C., Drage, T. C., and Snape, C. E. (2014b). Performance of polyethyleneimine-silica adsorbent for post-combustion CO_2 capture in a bubbling fluidized bed. *Chemical Engineering Journal*, 251:293 – 303.

Zhao, W., Zhang, Z., Li, Z., and Cai, N. (2013a). Continuous CO_2 capture in dual fluidized beds using silica supported amine. *Energy Procedia*, 37(0):89 – 98.

Zhao, W., Zhang, Z., Li, Z., and Cai, N. (2013b). Investigation of thermal stability and continuous CO_2 capture from flue gases with supported amine sorbent. *Industrial & Engineering Chemistry Research*, 52(5):2084–2093.